Rejection of two-photon fluorescence background in thick tissue by differential aberration imaging

Aymeric Leray, Jerome Mertz

Department of Biomedical Engineering, Boston University, 44 Cummington St., Boston, MA 02215

aleray@bu.edu, jmertz@bu.edu

Abstract: We present a simple and robust way to reject out-of-focus background when performing deep two-photon excited fluorescence (TPEF) imaging in thick tissue. The technique is based on the use of a deformable mirror (DM) to introduce illumination aberrations that preferentially degrade TPEF signal while leaving TPEF background relatively unchanged. A subtraction of aberrated from unaberrated images leads to background rejection. We present a heuristic description of our technique, which we corroborate with experiment. An added benefit of our technique is that it leads to somewhat improved image resolution.

OCIS codes: (170.6900) Three-dimensional microscopy; (190.4180) Multiphoton processes; (230.6120) Spatial light modulators.

References and links

1. W. Denk, J. H. Strickler, W. W. Webb, "Two-photon laser scanning fluorescence microscopy," Science **248**, 73-76 (1990).
2. F. Helmchen and W. Denk, "Deep tissue two-photon microscopy," Nat. Meth. **2**, 932-940 (2005).
3. K. Svoboda and R. Yasuda, "Principles of two-photon excitation microscopy and its applications to neuroscience," Neuron **50**, 823-829 (2006).
4. M. Oheim, E. Beaurepaire, E. Chaigneau, J. Mertz, S. Charpak, "Two-photon microscopy in brain tissue: parameters influencing the imaging depth," J. Neurosci. Meth. **111**, 29-37 (2001).
5. E. Beaurepaire and J. Mertz, "Epi-fluorescence collection in two-photon microscopy," Appl. Opt. **41**, 5376-5382 (2002).
6. E. Beaurepaire, M. Oheim, J. Mertz "Ultra-deep two-photon fluorescence excitation in turbid media," Opt. Commun. **188**, 25-29 (2001).
7. P. Theer, M. T. Hasan, W. Denk, "Two-photon imaging to a depth of 1000μm in living brains by use of a Ti:Al2O3 regenerative amplifier," Opt. Lett. **28**, 1022-1024 (2003).
8. J. Ying, F. Liu, R. R. Alfano, "Spatial distribution of two-photon-excited fluorescence in scattering media," Appl. Opt. **38**, 224-229 (1999).
9. M. A. A. Neil, R. Juskaitis, M. J. Booth, T. Wilson, T. Tanaka, S. Kawata, "Adaptive aberration correction in a two-photon microscope", J. Microsc. **200**, 105-108 (2000).
10. P. Marsh, D. Burns, J. Girkin, "Practical implementation of adaptive optics in multiphoton microscopy", Opt. Express **11**, 1123-1130 (2003).
11. D. Oron and Y. Silberberg, "Spatiotemporal coherent control using shaped, temporally focused pulses," Opt. Express **13**, 9903-9908 (2005).
12. G. Zhu, J. van Howe, M. Durst, W. Zipfel, C. Xu, "Simultaneous spatial and temporal focusing of femtosecond pulses," Opt. Express **13**, 2153-2159 (2005).
13. E. Tal, D. Oron, Y. Silberberg "Improved depth resolution in video-rate line-scanning multiphoton microscopy using temporal focusing," Opt. Lett. **30**, 1686-1688 (2005).
14. M. Born and E. Wolf, *Principles of Optics* (Cambridge University Press, Cambridge, UK, 1999).

#74520 - $15.00 USD Received 29 August 2006; revised 17 October 2006; accepted 20 October 2006

15. C. W. McCutchen, "Generalized aperture and the three-dimensional diffraction image," J. Opt. Soc. Am. **54**, 240-244 (1964).
16. B. R. Frieden, "Optical transfer of the three-dimensional object," J. Opt. Soc. Am. **57**, 56-66 (1967).
17. J. W. Goodman, *Introduction to Fourier Optics*, Roberts & Company Publishers, Greenwood Village, CO (2005).
18. J. Mertz, C. Xu, W. W. Webb, "Single-molecule detection by two-photon-excited fluorescence," Opt. Lett. **20**, 2532-2534 (1995).
19. J. Perreault, T. G. Bifano, B. Martin Levine, M. N. Horenstein, "Adaptive optic correction using microelectromechanical deformable mirrors," Opt. Eng. **41**, 561-566 (2002)
20. R. Heintzmann, V. Sarafis, P. Munroe, J. Nailon, Q. S. Hanley, T. M. Jovin, "Resolution enhancement by subtraction of confocal signals taken at different pinhole sizes," Micron **34**, 293-300 (2003).
21. E. Frumker, D. Oron, D. Mandelik, Y. Silberberg, "Femtosecond pulse-shape modulation at kilohertz rates," Opt. Lett. **29**, 890-892 (2003).

1. Introduction

Because two-photon excited fluorescence (TPEF) is dominantly generated by ballistic (unscattered) light, TPEF microscopy maintains high resolution even within scattering media [1, 2, 3]. According to Beer's law, the proportion of ballistic light arriving at the focus decays roughly exponentially with focal depth in the media. Hence, the laser power must be increased exponentially to maintain a relatively constant TPEF signal level at increasing imaging depths, and the depth limitation in TPEF microscopy is often limited simply by the maximum laser power available. Strategies to further increase depth penetration have included improving widefield fluorescence collection [4, 5] and temporally redistributing the laser power into high-energy pulses [6, 7]. This has revealed yet another limitation to depth penetration, namely that from out-of-focus fluorescence background generated at superficial tissue layers [8, 7]. This limitation arises when superficial background fluorescence, even though it is generated by a spatially extended laser beam, begins to dominate the deep signal fluorescence generated at the laser focus where the ballistic power has been weakened by scattering. Superficial background fluorescence can be all the more problematic when fluorophore labeling is dense, or when exposed or damaged tissue at the surface generates significant autofluorescence.

We propose a simple technique to reject out-of-focus TPEF background in scattering tissue. Our technique is based on the use of a deformable mirror to control the phase profile of the laser beam in the back aperture of the focusing objective. While most TPEF applications involving deformable mirrors aim at improving the quality of a laser-beam focus in thick tissue using adaptive optics [9, 10], our strategy is just the opposite: we purposefully degrade the quality of the focus by introducing extraneous aberrations. We argue that because TPEF is a nonlinear phenomenon, these aberrations dominantly quench in-focus TPEF signal while leaving out-of-focus TPEF background relatively unchanged. Out-of-focus TPEF background can therefore be effectively rejected by simple image subtraction.

A similar subtraction technique has been recently proposed in the temporal domain to improve the axial resolution of a TPEF microscope [11]. This technique is based on a re-shaping of laser pulses leading to temporal focusing [12, 13] or defocusing. The technique we introduce here does not rely on temporal reshaping, and indeed our discussion considers the spatial domain only. We present a heuristic description of our technique which we corroborate with experiment.

2. Formalism

Our goal in this paper is to provide a qualitative description of our technique, and we begin by considering an idealized sample where the fluorophore concentration is relatively uniform throughout the sample. The basic layout of our microscope is the same as that of a conventional TPEF microscope except that a deformable mirror is placed in a plane conjugate to the objective

#74520 - $15.00 USD Received 29 August 2006; revised 17 October 2006; accepted 20 October 2006

back focal plane, allowing control over the pupil aberrations. We consider imaging in a thick tissue and explicitly separate scattered from ballistic light by writing the *ballistic* laser intensity distribution in the tissue as

$$I_b(\vec{\rho},z) = W(z)PSF(\vec{\rho},z) \tag{1}$$

where $\vec{\rho}$ and z are coordinates relative to the laser beam focus (i.e. the surface of the sample is located at a negative z). This is the surviving portion of the laser intensity that has not incured scattering on its passage to depth z. The lateral beam profile is written as $PSF(\vec{\rho},z)$, which we normalize to $\int PSF(\vec{\rho},z)d^2\vec{\rho} = 1$ for all z. The total *ballistic* laser power at depth z is then simply $W(z)$. If we assume that all the ballistic light travels approximately the same optical path-length through the tissue to attain depth z, then $W(z)$ is subject to Beer's law and decays exponentially with increasing z. This small-angle assumption is equivalent to the paraxial approximation, which is valid for moderate to low numerical aperture (NA$\lesssim 0.7$). Within this approximation, we can interpret $PSF(\vec{\rho},z)$ as the ballistic point-spread-function, corresponding to profile of the laser beam if it were traveling through a perfectly transparent medium.

To address the issue of aberrations, we must examine not only the intensity distribution of the laser beam, but also the complex field distribution. Similarly as above, we define the ballistic coherent spread function $CSF(\vec{\rho},z)$ as the field distribution in a perfectly transparent medium. In the paraxial (Fresnel) approximation, this can be written as [14]

$$CSF(\vec{\rho},z) = \frac{1}{(2\pi)^2}e^{ikz}\int\left(P(\vec{k}_\perp)e^{-iz\frac{k_\perp^2}{2k}}\right)e^{i\vec{\rho}\cdot\vec{k}_\perp}d^2\vec{k}_\perp \tag{2}$$

from which we obtain

$$PSF(\vec{\rho},z) = \frac{|CSF(\vec{\rho},z)|^2}{\int|CSF(\vec{\rho},z)|^2\,d^2\vec{\rho}} \tag{3}$$

In Eq. (2) $k = 2\pi/\lambda$ where λ is the mean laser wavelength, and we have introduced the pupil function $P(\vec{k}_\perp)$ whose Fourier coordinates $\vec{k}_\perp$ are located in the objective back focal plane (or, equivalently, the DM plane). The expression in parentheses in Eq. (2) may be regarded as a generalized 3D pupil function [15, 16]. The purpose of the DM in our case will be to introduce controlled aberrations $\phi(\vec{k}_\perp)$ in the objective pupil such that

$$P_\phi(\vec{k}_\perp) = P_0(\vec{k}_\perp)e^{i\phi(\vec{k}_\perp)} \tag{4}$$

where the subscripts ϕ and 0 refer to DM-aberrated and unaberrated (i.e. diffraction-limited) pupils respectively. It is straightforward to demonstrate that $\int PSF_\phi(\vec{\rho},z)d^2\vec{\rho} = 1$ regardless of $\phi(\vec{k}_\perp)$. Moreover, assuming that $\phi(\vec{k}_\perp)$ does not deviate the ballistic light rays to the point of invalidating the paraxial approximation, then $W_\phi(z) \approx W_0(z)$ for all z. The latter is a statement that aberrations in the pupil do not globally affect the net ballistic power of the laser light in the tissue, which is defined by the scattering properties of the tissue alone.

3. Effect of aberrations on TPEF

For the simple model presented here, we adopt the generally accepted principle that TPEF is dominantly generated by ballistic excitation [2]. This principle is one of the defining characteristics of TPEF and arises specifically from its nonlinear nature (conditions where this principle might break down are discussed in the conclusion). We write then

$$F(z) = W^2(z)\int PSF^2(\vec{\rho},z)d^2\vec{\rho} \tag{5}$$

#74520 - $15.00 USD Received 29 August 2006; revised 17 October 2006; accepted 20 October 2006

where $F(z)$ is the TPEF power generated at depth z and we have dropped prefactors such as fluorophore concentration (which is considered to be uniform here), cross-section, etc.. We have also dropped any consideration of the temporal profile of the laser pulses since we will only consider DM strokes that are much smaller than the laser coherence length.

Alternatively, we may express the TPEF power generated at depth z in terms of the 2D ballistic optical transfer function, defined by

$$OTF(\vec{k}_\perp;z) = \int PSF(\vec{\rho},z)e^{i\vec{\rho}\cdot\vec{k}_\perp}d^2\vec{\rho} \tag{6}$$

which, from Parseval's theorem, leads to:

$$F(z) = \frac{W^2(z)}{(2\pi)^2}\int \left|OTF(\vec{k}_\perp;z)\right|^2 d^2\vec{k}_\perp \tag{7}$$

It is well known that any introduction of aberrations in the objective pupil leads to a degradation in the transfer of optical frequencies to the focal plane. From Schwarz's inequality[17], we obtain $\left|OTF_\phi(\vec{k}_\perp;0)\right| \leq \left|OTF_0(\vec{k}_\perp;0)\right|$, from which we infer

$$F_\phi(0) \leq F_0(0) \tag{8}$$

In general, therefore, an introduction of DM-induced aberrations decreases the amount of TPEF produced at the focal plane, and hence quenches TPEF signal (note: we do not consider the possibility that DM-induced aberrations might, by chance, compensate for tissue-induced aberrations, as is usually desired in adaptive optics applications).

We further argue that these same aberrations have much less effect on out-of-focus TPEF background. That is

$$F_\phi(z) \to F_0(z) \quad \text{for large } |z|\,. \tag{9}$$

An initial motivation for our argument comes from examining Eqs. (2) and (4) and noting that in fact two aberrations act to degrade the ballistic laser profile: one aberration is induced by the DM ($\phi(\vec{k}_\perp)$) and another is induced simply by defocus ($zk_\perp^2/2k$). The latter worsens with increasing $|z|$ whereas the former does not since it is independent of z. We therefore expect that for large enough $|z|$, the effects of defocus dominate over those of DM-induced aberrations, meaning that DM-induced aberrations should have little influence on TPEF background for planes that are far out of focus.

A more intuitive interpretation of the effects of DM-induced aberrations comes from considering the depth-dependent lateral area of the ballistic laser light, defined by

$$Area(z) = \frac{\left(\int I_b(\vec{\rho},z)d^2\vec{\rho}\right)^2}{\int I_b^2(\vec{\rho},z)d^2\vec{\rho}} = \frac{(2\pi)^2}{\int \left|OTF(\vec{k}_\perp;z)\right|^2 d^2\vec{k}_\perp} \tag{10}$$

(This definition is a 2D area version of the 3D TPEF volume definition introduced in [18]). A pictoral representation of this area is illustrated in the inset of Fig. (1), where we sketch the profile of the ballistic laser light with (dashed) and without (solid) DM-induced aberrations. Assuming that the DM-induced aberrations do not significantly alter the convergence angle of the ballistic light in the sample, then from simple geometrical considerations it is clear that the relative change in the ballistic-beam area provoked by DM-induced aberrations is greater at the focal plane than away from the focal plane. Moreover, it is apparent that as $|z|$ becomes larger, this relative change in ballistic-beam area becomes less and less significant, particularly if the ballistic-beam convergence angle is tight. Because TPEF is a nonlinear phenomenon, the

#74520 - $15.00 USD Received 29 August 2006; revised 17 October 2006; accepted 20 October 2006

TPEF generated at depth z is highly dependent on the area of the ballistic beam at this depth. In particular, from Eqs.(1) and (10) we obtain the important relation

$$\frac{Area_\phi(z)}{Area_0(z)} = \frac{F_0(z)}{F_\phi(z)}. \tag{11}$$

We infer from this relation that the predicted effect of DM-induced aberrations is to quench TPEF near the beam focus while not significantly quenching it far from the focus, as anticipated from expressions (8) and (9). By performing a simple subtraction

$$\Delta F(z) = F_0(z) - F_\phi(z) \tag{12}$$

we then expect to reject out-of-focus TPEF background while preserving in-focus TPEF signal. This is the basic principle of our differential aberration imaging technique. The results here, derived qualitatively, are corroborated by experiment.

4. Experimental demonstrations

The layout of our microscope is shown in Fig. (1). This layout is the same as that of a standard TPEF microscope except that the incident laser beam is reflected from a DM prior to being scanned. Afocal lenses in the beam path are arranged such that the DM is in a plane conjugate to the back aperture of the objective. The DM consists of 12×12 reflecting elements, each $\sim400\mu$m in size (Boston Micromachines Corporation μDMS-Multi with a 3.5μm maximum stroke [19]). The total DM clear aperture is 4.4mm, which is roughly filled by the laser beam. When performing unaberrated imaging, the voltage applied to each actuator in the DM is set to zero, meaning that the DM is flat to within 40nm (rms), according to manufacturer specifications. When performing aberrated imaging, a predefined voltage pattern is applied to the DM actuators.

An advantage of our differential aberration imaging technique is that the DM is operated in an open-loop configuration. That is, the voltages applied to the DM actuators are not prescribed by feedback signals, as they would be in adaptive optics applications. The applied aberrations in our case need only degrade the focal spot profile, which is relatively easy to achieve. However, to ensure that the aberrated and unaberrated images are properly co-registered, the aberrated focal spot should lie roughly at the same location as the unaberrated focal spot. Constraints on the applied aberrations are therefore that they produce no defocus nor tilt to the illumination intensity. For our demonstrations, we applied voltages on the DM actuators to produce either 0 or π local phase shifts on the reflected beam. Two patterns, in particular, were investigated as shown in Fig (1). Both patterns have the advantage that they provoke no defocus (the 2-zone pattern, however, produces a slight tilt). Both patterns also lead to aberrations that are independent of the beam spot size incident on the DM. We chose to sub-divide the DM pattern into few zones rather than many zones so as to minimize beam divergence from the DM and ensure that the same amount of power is delivered to the sample with or without aberrations. This was verified in practice: the power delivered to the sample dropped by only 1% or 2% when the aberrations were introduced.

Our technique of background subtraction is based on the relations (8) and (9). The validity of these relations can be verified theoretically if we assume that the laser beam has a Gaussian profile and the objective aperture is large. In this case, the effects of the 4-zone and 2-zone aberrations on the illumination field can be calculated exactly, as can their effects on the resultant TPEF signal produced by an infinitely thin uniform fluorescent plane. To confirm these results experimentally, we monitored the TPEF signal from a thin fluorescent slab with and without induced aberrations as a function of defocus. Plots of $F_0(z)$ and $F_\phi(z)$ and of their ratio, both

#74520 - $15.00 USD Received 29 August 2006; revised 17 October 2006; accepted 20 October 2006

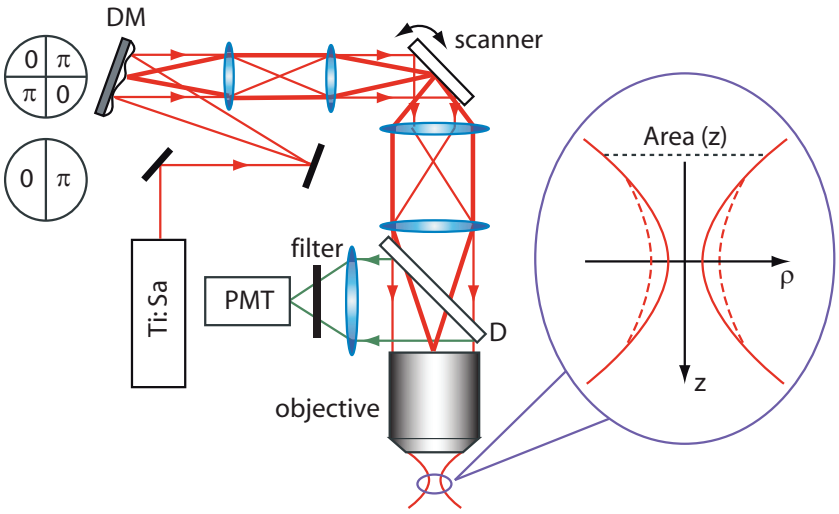

Fig. 1. Experimental layout. A mode-locked Ti:sapphire laser beam is focused into a sample, and the resulting TPEF is detected in the backward direction with photomultiplier tube (PMT). The layout is the same as a standard TPEF microscope except that a DM has been inserted into the beam path prior to the scan mirrors (4mm clear aperture). A set of unit-magnification afocal lenses image the DM to the scan mirrors (and hence to the objective back aperture). Aberrations are applied by 4-zone or 2-zone voltage patterns at the DM, as shown. The inset is a schematic of the ballistic-light focus profile in the sample without (solid) and with (dashed) DM-induced aberrations. The aberrations provoke a relative increase in the cross-sectional area of this profile (and hence a relative decrease in TPEF) that is more pronounced near the focal plane than far from the focal plane.

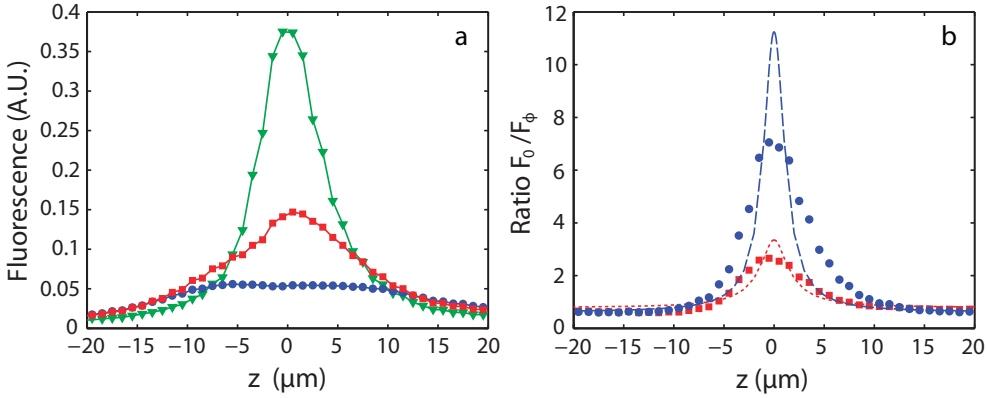

Fig. 2. Plots of TPEF from a thin uniform fluorescent slab (˜6μm thick fluorescein solution sandwiched between two coverslips) as a function of defocus. Measurements were taken without (green triangles) and with 2-zone (red squares) and 4-zone (blue circles) DM-induced aberrations. (a) Plots of $F_0(z)$ (green) and $F_\phi(z)$ (red, blue) and, (b) the corresponding ratios $F_0(z)/F_\phi(z)$. Measurements were acquired with no beam scanning and an Olympus 20× NA=0.95 objective. Dashed traces in (b) are theoretical evaluations of $F_0(z)/F_\phi(z)$ for an infinitely thin fluorescent plane.

#74520 - $15.00 USD Received 29 August 2006; revised 17 October 2006; accepted 20 October 2006

theoretical and experimental, are illustrated in Fig. (2). As anticipated, $F_0(z)/F_\phi(z)$ is larger than unity near focus and decays approximately toward unity away from focus, confirming the relations (8) and (9) required for our technique. From Eq. (11), this decay toward unity also confirms our intuitive picture that the laser-beam area remains relatively unaffected by aberrations far away from focus, at least for the aberrations tested here. We note that the experimental ratio plots exhibit smaller peak heights and greater peak widths than anticipated by theory. This is largely due to the fact that our fluorescent slab was not infinitely thin. Fig. 2a also reveals that the ratio $F_0(z)/F_\phi(z)$ actually falls below unity, indicating that 4-zone and 2-zone aberrations apparently lead to a small increase in fluorescence background. This increase is corroborated by theory and subsists for several tens of microns. Presumably, this small increase arises from the fact that the aberrated beam profile is not as smooth as the unaberrated (Gaussian) beam profile, causing the eventual convergence $F_0(z)/F_\phi(z) \to 1$ to be slow.

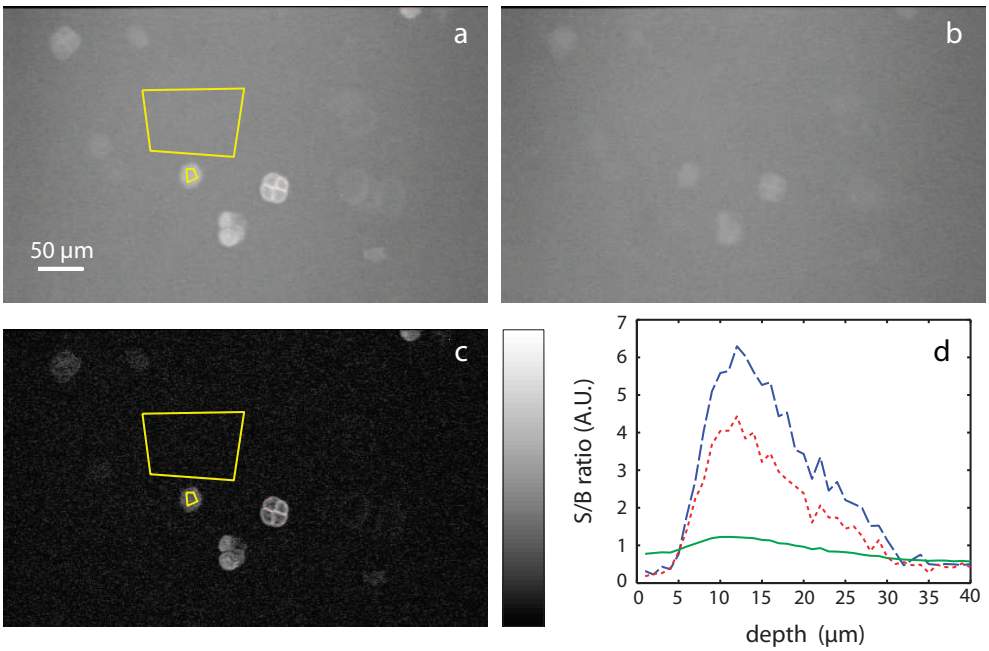

Fig. 3. Demonstration of TPEF background subtraction by differential aberration imaging. A thick tissue sample was mimicked by artificially rendering the objective immersion medium (water-ethanol mixture) both scattering and uniformly fluorescent, resulting in significant TPEF background (the medium scattering length was $\sim 500\mu$m and the Olympus 20$\times$ NA=0.95 objective working distance was 2mm). Images of fluorescently labeled pollen grains (Carolina Biological Supply) were acquired without (a) and with (b) 4-zone DM-induced aberrations (same lookup table). Upon subtraction (c), the background is considerably reduced and the contrast of the pollen grains is enhanced (same lookup table, but autoscaled). Note: for clearer images, averaging was performed over a 10 frame z-stack spanning a 10μm depth; negative values in panel (c) were set to zero post averaging. Qualitative measures of contrast improvement are shown in panel (d) illustrating the ratio of signal+background (averaged over a small zone inside a pollen grain) to background (averaged over a zone in proximity of the pollen grain). The ratio is shown for the uncorrected image (solid green), and after differential aberration correction with 2-zone (dotted red), and 4-zone (dashed blue) aberrations. The depth$=0$ reference is arbitrary. The images were obtained with a laser power of $\sim$70mW (after the objective) at $\lambda = 800$nm.

#74520 - $15.00 USD Received 29 August 2006; revised 17 October 2006; accepted 20 October 2006

For practical TPEF imaging applications, the advantages of background subtraction become most apparent when significant background is generated at out-of-focus planes. As argued above this can happen when performing very deep imaging in scattering tissue, particularly when the fluorophores in the tissue are roughly uniformly distributed and of high density, or, worse still, if the tissue exhibits strong (auto)fluorescence at its surface. The laser used in our experiments was low power (Spectra-Physics Tsunami pumped by a 5W Millennia), not particularly appropriate for very deep imaging. For demonstration purposes we chose to mimic the conditions described above with an artificial test sample. The sample consisted of fluorescently labeled pollen grains under a microscope coverslip. These were imaged with a water- immersion objective. By dissolving rhodamine dye and TiO_2 particles in the immersion medium (a water-ethanol mixture in this case), and choosing the concentrations of each appropriately, conditions could readily be attained where the signal from the pollen grains became dominated by background from the immersion medium. As shown in Fig. (3), the pollen grains became barely visible when performing normal TPEF imaging (i.e. no aberrations). However, upon differential aberration background subtraction the contrast of the pollen grains was indeed markedly improved. Plots of this contrast improvement for different induced aberration patterns are shown in Fig. (3d).

An auxiliary benefit of our background subtraction technique is that it somewhat improves image resolution, as qualitatively illustrated in Fig. (4). Similar ideas of using background subtraction to improve image resolution have been previously demonstrated with different techniques. For example, an improvement in TPEF axial resolution was demonstrated by differential temporal focusing [11]. Alternatively, an improvement in lateral resolution was demonstrated in simple confocal microscopy by differential pinhole-size imaging [20]. In all cases the principle of resolution improvement is the same: background subtraction preferentially quenches the out-of-focus wings of the imaging point-spread-function, thereby effectively causing it to be narrower.

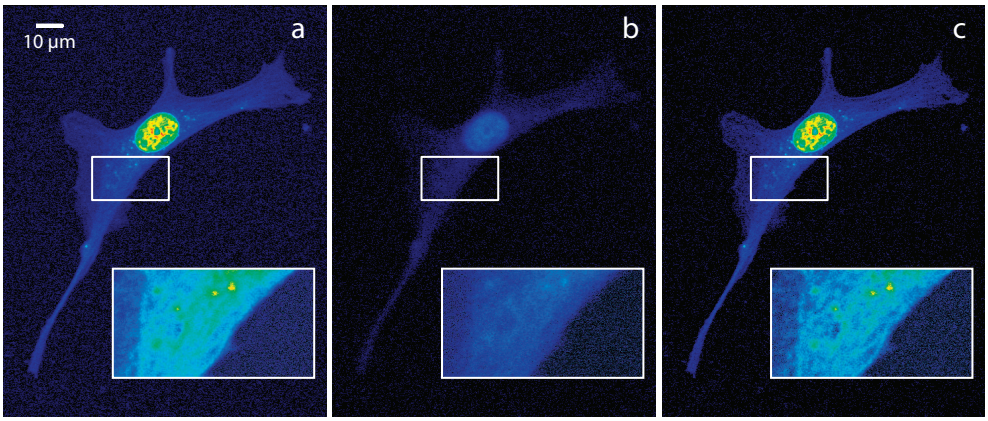

Fig. 4. Illustration of the resolution enhancement occasioned with differential aberration TPEF imaging. A fixed multiply-labeled bovine pulmonary artery endothelial cell (Molecular Probes Fluocell) was imaged without (a) and with (b) 4-zone DM-induced aberrations, and their subtraction is shown in (c). The higher magnification insets were acquired at higher laser power. The resolution of the Bodipy-labeled microtubules in these insets is apparently enhanced upon image subtraction. Images were acquired with an Olympus 40× NA=1.3 oil immersion objective. The immersion medium here was neither scattering nor fluorescent.

#74520 - $15.00 USD Received 29 August 2006; revised 17 October 2006; accepted 20 October 2006

5. Conclusion

In conclusion, we have demonstrated a differential aberration imaging technique to reject out-of-focus background in TPEF imaging of thick tissue. An added benefit of our technique is that it somewhat improves 3D resolution. The technique is robust because the exact nature of the induced aberrations need not be precisely controlled.

We note that in our treatment here we have assumed that TPEF background is generated exclusively by out-of-focus ballistic excitation. While this is largely true when the fluorophore density throughout the scattering sample is high, or when there is significant superficial (auto)fluorescence, it becomes less true when the fluorophore density is sparse. In this last case, the scattered excitation near the focal plane rather than the ballistic excitation away from the focal plane may become the dominant contributor of TPEF background. Our differential aberration imaging technique continues to help in this case, however with reduced benefits (a theoretical treatment of these benefits will be presented elsewhere).

For the demonstrations presented here, background subtraction was performed frame by frame. This may not be suitable in cases where motion in the sample occurs on time scales faster than the frame rate. We therefore plan to improve our technique by developing a faster aberration modulation mechanism and performing background subtraction line by line rather than frame by frame. In this manner, background will be acquired during scanner flyback and the overall image acquisition rate will not be significantly impaired compared to that of a standard TPEF microscope. An example of a fast modulation scheme has been proposed for femtosecond pulse-shaping [21].

Finally, we note that DM's are generally intended to improve rather than degrade laser focus quality when applied in scanning microscope configurations. Our technique of background subtraction is entirely compatible with this philosophy. Ideally, for better results than those presented here, the signal image could be optimized with adaptive optics prior to background subtraction. However, this would prescribe a much greater level of sophistication to what is currently a very simple technique. As it stands, our technique is robust and easy to implement and can be of general use in TPEF imaging.

Acknowledgments

This work was funded by the Whitaker Foundation and by the NIH (R21EB005736). We are indebted to Boston Micromachines Corporation for loaning us a deformable mirror, without which this work would not have been done.

#74520 - $15.00 USD Received 29 August 2006; revised 17 October 2006; accepted 20 October 2006